



HAL
open science

The hydroxymethylome of multiple myeloma identifies FAM72D as a 1q21 marker linked to proliferation

Fabrice Chatonnet, Amandine Pignarre, Aurelien Serandour, Gersende Caron,
Stéphane Avner, Nicolas Robert, Alboukadel Kassambara, Audrey Laurent,
Maud Bizot, Xabier Agirre, et al.

► To cite this version:

Fabrice Chatonnet, Amandine Pignarre, Aurelien Serandour, Gersende Caron, Stéphane Avner, et al..
The hydroxymethylome of multiple myeloma identifies FAM72D as a 1q21 marker linked to proliferation. *Haematologica*, 2020, 105 (3), pp.774-783. 10.3324/haematol.2019.222133 . hal-02165596

HAL Id: hal-02165596

<https://univ-rennes.hal.science/hal-02165596v1>

Submitted on 18 Oct 2019

HAL is a multi-disciplinary open access archive for the deposit and dissemination of scientific research documents, whether they are published or not. The documents may come from teaching and research institutions in France or abroad, or from public or private research centers.

L'archive ouverte pluridisciplinaire **HAL**, est destinée au dépôt et à la diffusion de documents scientifiques de niveau recherche, publiés ou non, émanant des établissements d'enseignement et de recherche français ou étrangers, des laboratoires publics ou privés.

Copyright

The hydroxymethylome of multiple myeloma identifies *FAM72D* as a 1q21 marker linked to proliferation

Running title: The hydroxymethylome of multiple myeloma

Fabrice Chatonnet,^{1,§} Amandine Pignarre,^{1,§} Aurélien A Sérandour,^{2-3-4,§} Gersende Caron,¹ Stéphane Avner,⁵ Nicolas Robert,⁶ Alboukadel Kassambara,⁷ Audrey Laurent,⁵ Maud Bizot,⁵ Xabier Agirre,⁸ Felipe Prosper,⁸ José I Martin-Subero,⁹ Jérôme Moreaux,^{6-7,*} Thierry Fest,^{1,*} and Gilles Salbert^{5,*}

¹Université Rennes 1, CHU Rennes, Inserm, MICMAC - UMR_S 1236, F-35000 Rennes, France.

²CRCINA, INSERM, CNRS, Université d'Angers, Université de Nantes, Nantes, France

³Ecole Centrale de Nantes, Nantes, France

⁴Institut de Cancérologie de l'Ouest, Site René-Gauducheau, Saint-Herblain, France

⁵SPARTE, IGDR, CNRS UMR6290, University Rennes 1, Rennes, France

⁶Department of Biological Hematology, CHU Montpellier, Montpellier, France

⁷IGH, CNRS, Univ Montpellier, France

⁸Area de Oncología, Centro de Investigación Médica Aplicada (CIMA), Universidad de Navarra, Pamplona, Spain.

⁹IDIBAPS, Barcelona, Spain

[§] These authors contributed equally to this work.

* Corresponding authors:

- Gilles Salbert, email: gilles.salbert@univ-rennes1.fr, tel: +33 (0)2 23 23 66 25, fax: +33 (0)2 23 23 67 94

- Thierry Fest, email: thierry.fest@univ-rennes1.fr, tel: +33 (0)2 99 28 42 72, fax: +33 (0)2 99 28 41 52

- Jérôme Moreaux, email: jerome.moreaux@igh.cnrs.fr, tel: +33 (0)4 67 33 79 03, fax: +33 (0)4 67 33 70 36

Keywords: Multiple myeloma, DNA methylation, 5hmC, FOXM1, FAM72

Abstract

Cell identity relies on the cross-talk between genetics and epigenetics and their impact on gene expression. Oxidation of 5-methylcytosine into 5-hydroxymethylcytosine is the first step of an active DNA demethylation process occurring mainly at enhancers and gene bodies and, as such, participates in processes governing cell identity in normal and pathological conditions. Although genetic alterations are well documented in multiple myeloma, epigenetic alterations associated with this disease have not yet been thoroughly analyzed. To gain insight into the biology of multiple myeloma, genome-wide 5-hydroxymethylcytosine profiles were obtained and showed that regions enriched in this modified base overlap with multiple myeloma enhancers and super enhancers and are close to highly expressed genes. Through the definition of a multiple myeloma-specific 5-hydroxymethylcytosine signature, we identified *FAM72D* as a poor prognostic gene located on 1q21, a region amplified in high risk myeloma. We further uncovered that *FAM72D* functions as part of the *FOXM1* transcription factor network controlling cell proliferation and survival and evidenced an increased sensitivity of cells expressing high levels of *FOXM1* and *FAM72* to epigenetic drugs targeting histone deacetylases and DNA methyltransferases.

Introduction

Multiple myeloma (MM) is a genetically and clinically heterogeneous hematological cancer associated with a limited number of gene translocations into the immunoglobulin heavy chain locus of plasma cells (PCs). In particular, *CCND1*, *CCND3*, *c-MAF*, *MAFB* and *MMSET* translocations influence prognosis and are used to classify patients into molecular subgroups.¹ Genome sequencing studies have revealed considerable heterogeneity and genomic instability, a complex mutational landscape and a branching pattern of clonal evolution.^{2,3} Epigenetic modifications including DNA methylation and histone modifications have been also related to MM pathophysiology.⁴⁻⁶ Patients with highly proliferative PCs can also show genetic instability of the chromosome 1q arm and specially of the pericentromeric region 1q12 and of its immediate neighbor 1q21.^{7,8} Amplification of 1q21, and possibly overexpression of genes lying in 1q21, parallel disease progression.⁸ However, no causal link between proliferation and 1q21 instability has yet been demonstrated, although overexpression of the histone chaperone gene *ANP32E*, in 1q21.2 and the cyclin-dependent kinase regulator *CKS1B*, in 1q21.3, is of poor prognosis in MM.⁹ More recently, *ILF2*, in 1q21.3, was proposed to be involved in the pathogenic role of 1q21 amplification by increasing DNA damage resistance.¹⁰ Nonetheless, other yet

unidentified genes might participate in the pathogenicity of 1q21 gain.

Tumor PC clones show different levels of differentiation,¹¹ suggesting that MM could originate either from B cells that do not fulfill a complete differentiation program, or from PCs that partially dedifferentiate. Cell differentiation relies on the selective engagement of small genomic regions called enhancers which are bound by transcription factors (TFs) controlling cell-specific transcriptional programs. As an early step of activation, enhancers undergo active DNA demethylation through iterative oxidation of 5-methylcytosine (5mC) into 5-hydroxymethylcytosine (5hmC), 5-formylcytosine (5fC) and 5-carboxylcytosine (5caC) by Ten-Eleven-Translocation (TET) enzymes and repair by the base excision repair machinery, including the T:G mismatch DNA glycosylase TDG which cleaves 5fC and 5caC.¹² 5hmC has been mapped genome-wide in several cell differentiation models, including *in vitro* differentiation of human naive B cells (NBCs) into plasmablasts, where 5hmC accumulates at PC identity genes, as well as in mouse germinal center B cells.¹³⁻¹⁵ These studies showed enrichment in 5hmC at poised/active enhancers as well as in the body of highly transcribed genes. Despite the wealth of information on the genetics of MM, the epigenetics of this disease is still poorly described. Nonetheless, a recent genome-wide investigation of active chromatin regions showed that opening of heterochromatin is a hallmark of MM.¹⁶ In addition, interrogation of DNA methylation in MM cells revealed that, despite a global hypomethylation, their genome shows specific hypermethylation of enhancers that normally undergo complete demethylation during B cell commitment and are bound by B cell TFs.¹⁷ Interestingly, the methylation levels of these enhancers were anti-correlated with expression levels of B cell-specific TFs in MM patients,¹⁷ suggesting that variations in tumor PC differentiation states could indeed be controlled through DNA methylation/demethylation mechanisms guided by specific TFs. Here, we investigated the genome-wide distribution of 5hmC in tumor PCs and, through the identification of MM-specific hydroxymethylated regions, evidenced new prognosis genes that might contribute to the understanding of this disease.

Methods

Primary multiple myeloma cells

Bone marrow samples were collected after patients' written informed consent in accordance with the Declaration of Helsinki and institutional research board approval from Montpellier University hospital. Patients' MM cells were purified using anti-CD138 MACS microbeads (Miltenyi Biotech, Bergisch Gladbach, Germany).

RNA and genomic DNA were extracted using Qiagen kits (Qiagen, Hilden, Germany) and their gene expression profile (GEP) obtained using Affymetrix U133 plus 2.0 microarrays as described.¹⁸ Plasma cell labeling index (PCLI)¹⁹ was investigated using BrdU incorporation and flow cytometry in 101 patients at diagnosis. Correlation between gene expression and PCLI was determined with a Spearman's test. We used publicly available Affymetrix GEP (Gene Expression Omnibus, accession number GSE2658) of a cohort of 345 purified MM cells from previously untreated patients from the University of Arkansas for Medical Sciences (UAMS, Little Rock, AR), termed in the following UAMS-TT2 cohort. These patients were treated with total therapy 2 including HDM and ASCT.²⁰ We also used Affymetrix data from total therapy 3 cohort (UAMS-TT3; n=158; E-TABM-1138)²¹ of 188 relapsed MM patients subsequently treated with bortezomib (GSE9782) from the study by Mulligan et al.²²

FDI-6 treatment of primary MM cells from patients

BM of patients presenting with previously untreated MM (n=6) at the university hospital of Montpellier was obtained after patients' written informed consent in accordance with the Declaration of Helsinki and agreement of the Montpellier University Hospital Centre for Biological Resources (DC-2008-417). Mononuclear cells were treated with or without graded concentrations of FDI-6 and MM cells cytotoxicity was analyzed using anti-CD138-phycoerythrin monoclonal antibody (Immunotech, Marseille, France) as described previously.⁵

Genome-wide mapping of 5-hydroxymethylcytosine and bioinformatics

5hmC was mapped by selective chemical labeling,²³ coupled or not with exonuclease digestion,^{24,25} of 10 µg of sonicated (Bioruptor, Diagenode) genomic DNA from MM patients or from MCF-7 cells. Libraries were obtained using the TruSeq ChIP Sample Prep Kit (Illumina), quantified using the KAPA library quantification kit (KAPA Biosystems) and 50 bp single end sequenced with HiSeq 1500 (Illumina). Reads were mapped to hg19 and processed as described.²⁵ SCL-exo signal was normalized to the input signal. Principal component analyses (PCA) were run online with Galaxy (<http://deeptools.ie-freiburg.mpg.de/>) with 5hmC signal binned by 10 kb windows. Heatmap clustering of hydroxymethylated CpGs was run online (<http://cistrome.org/>).²⁶ Search for transcription factor binding site (TFBS) motifs surrounding hydroxymethylated CpGs used the online *Centdist* tool²⁷ in 600 bp windows centered on 5hmCpGs. Annotation of 5hmCpGs used GREAT.²⁸ Oxidative bisulfite modification of gDNA and hybridization to Illumina 450K arrays were run as previously described.²⁹ ChIP-seq

data for H3K27ac in primary MM cells¹⁶ were downloaded from the European Nucleotide Archive database (PRJEB25605). Data were deposited in the Gene Expression Omnibus database under accession number GSE124188.

A detailed description of additional methods is available in supplemental information.

Results

5hmC-enrichment partly recapitulates the molecular classification of MM

To better understand the relationship between DNA demethylation processes and cell identity in MM, we generated genome-wide maps of 5hmC in MM cells isolated from 11 patients belonging to different molecular subgroups, as well as for 3 human myeloma cell lines (HMCLs), either by SCL-exo^{24,25} or SCL-seq²³ (Fig. 1A). In parallel, 10 MM samples were processed through the oxidative-bisulfite modification procedure and hybridized to Illumina 450K arrays (oxBS-450K).²⁹ Annotation of 5hmC positive regions (40,586 CpGs for oxBS-450K; 86,591 CpGs for SCL-exo; 64,424 regions for SCL-seq) aggregated from all patients included in each procedure was run using GREAT.²⁸ Results indicated that oxBS-450K did not generate meaningful information whereas SCL-exo and SCL-seq highlighted characteristics of PC biology such as endoplasmic reticulum stress, immune response, but also pathways which could be linked to MM, such as "IRF4 target genes"³⁰ (Supplemental Fig. S1A). Based on these annotation data, only SCL-exo and SCL-seq identified regions were further analyzed. Results were first compared to genome-wide 5hmC maps of naive B cells and plasmablasts previously generated by SCL-seq.¹⁴ Principal component analysis (PCA) of the signal showed dispersion of the samples, suggesting variability between tumor hydroxymethylomes. Nonetheless, most MM hydroxymethylomes grouped closer to PBs than to NBCs (Fig. 1B). When running PCA only with MM patients from the MMSET, CCND1 and Proliferation groups, 3 clusters were observed (C1 to C3 Fig. 1B). These clusters gathered together patients from similar molecular groups, although two patients did not follow this rule (E12097 and E6068), indicating that molecular groups are probably heterogeneous in nature and that 5hmC maps can help refine molecular clustering. We next generated the union of significantly hydroxymethylated CpGs ($p < 5e^{-2}$) overlapping between samples within each cluster. These 6,385 individual CpGs were clusterized according to their 5hmC levels (Fig. 1C). The resulting heatmap evidenced two groups of CpGs that were selectively more hydroxymethylated either in C1 patients (C'1 cluster) or in C2 patients (C'2 cluster). Analysis of motif enrichment for transcription factor binding sites in C'1 and C'2 and their comparison with motifs found in NBC and PB hydroxymethylated regions

suggested that MM cells from C2 patients remain more differentiated than those from C1 patients. Indeed, the BLIMP1 (a major regulator of PC differentiation) motif was significantly enriched in C'2 but not in C'1 regions (Supplemental Fig. S1B). Accordingly, functional annotation through GREAT showed that C'2 regions associated with endoplasmic reticulum stress gene signature or IL-6 signaling, features of mature PC, whereas C'1 regions did not (Fig. 1C). Conversely, NOTCH, MYC, Cell Cycle and BCR signaling, which are more characteristic of proliferating and/or undifferentiated B cells, were significantly more associated with C'1 regions than with C'2 regions (Fig. 1C). Of note, the SUH and GLI motifs were also selectively enriched in C'1 regions (Supplemental Fig. S1B). Hence, C1 patients from the proliferation group probably have active NOTCH and SHH pathways, both important for proliferation of CD138⁺ MM cells.³¹⁻³² In addition, the binding motif for MEIS1, a known regulator of hematopoietic progenitor self-renewal³³, was also selectively enriched in C'1 regions. Collectively, these data indicate that MM cells from the proliferation group have an under-differentiated phenotype which proliferation is likely to rely on a MEIS1/SUH/GLI transcription factor cocktail as well as MYC activity. These results also show that 5hmC is indeed indicative of the biological and clinical traits of patients and could be used to delineate groups with different characteristics.

5mC oxidation targets MM plasma cell enhancers

Investigating the genomic location of high confidence MM 5hmCpGs (86,591 CpGs, $p < 1e^{-5}$) showed that they were mostly distributed in introns and distal intergenic regions and, as previously observed in NBCs, PBs and mouse activated B cells,^{14,15} genes which were close to a 5hmC enriched region showed higher expression than genes which had no such region in their vicinity (Fig. 2A). We next considered the presence of these 5hmCpGs in regions harboring different chromatin states (ChromHMM) and defined for the lymphoblastoid cell line GM12878 (a cell line used as a model of normal B cells) by the ENCODE consortium. In accordance with a proposed global opening of chromatin in MM cells and as already described for open chromatin regions in MM,¹⁶ and for MM hypomethylated CpGs,¹⁷ MM 5hmCpGs mainly reside in regions of heterochromatin in GM12878 cells (Supplemental Fig. S2A). During differentiation of NBCs into PBs, genomic sites undergoing 5mC oxidation often bear histone marks of either commissioned (H3K4me1) or active (both, H3K27ac and H3K4me1) enhancers.^{14,15} To interrogate the relation between 5mC oxidation and enhancers in MM, we next analyzed enrichment in H3K4me1 and H3K27ac from NBCs, PCs and MM cells around 5hmCpGs detected in MM patients. Most MM 5hmCpGs were found in PC and NBC H3K4me1-premarked genomic sites that become

active in MM (Fig. 2B). We next investigated the presence of MM 5hmCpGs in active enhancers and super-enhancers (SEs) identified in the MM1.S HMCL.³⁴ Most notably, 89.3% (275/308) of the active MM1.S SEs and 36% (2949/8285) of all active enhancers were enriched in 5hmCpGs in MM (Supplemental Fig. S2B), strongly suggesting a role for 5mC oxidation in the control of SE activity. Similar results were obtained when analyzing the overlap between 5hmCpGs and U-266 enhancers and SEs defined on the H3K27ac ChIP-seq signal from the Blueprint consortium (not shown). However, as exemplified for the *KLF13* SE (Fig. 2C), the vast majority (98.5%, 271 out of 275) of these MM1.S active SEs were already marked with 5hmC in PBs, indicating that these SEs probably maintain a cell-of-origin identity in MM cells. Nonetheless, 4 SEs showed a MM-specific hydroxymethylation profile, including 2 *DEPTOR* SEs, *MYC* SE and *GAS2* SE (Fig. 2C). *DEPTOR* and *MYC* are known to promote MM cell proliferation and survival^{4,35} and, in support of our data, their SEs were found to be specifically active in MM cells.¹⁶ *GAS2* has not been associated with MM yet but it has been shown to be upregulated and to favor survival in chronic myeloid leukemia cells in correlation with hypomethylation of its promoter region.^{36,37} When examined during NBC to PC differentiation (Supplemental Fig. S2C) as well as in patients of the Arkansas MM cohort (Supplemental Fig. S2D), *GAS2* mRNA levels were detected in BMPCs but found to be higher in MM cells. Furthermore, *GAS2* overexpression impacted patient survival (Fig. 2C). Since *GAS2* inhibits calpain proteases which degrade TET enzymes,³⁸ it could thus play a central role in sustaining 5mC oxidation levels in MM cells. Overall, this analysis indicates that 5mC oxidation in MM occurs mainly in intronic enhancers and participates in the establishment of a myeloma-specific gene expression program.

A MM-specific 5hmC signature identifies prognosis genes

We next delineated a MM-specific 5hmC signature, independently of molecular subgroups, through first calling CpGs that were hydroxymethylated ($p < 1e^{-5}$) in at least 33% of the myeloma samples and not falling into genomic regions hydroxymethylated in PBs ($p < 1e^{-2}$), and second by iterative clustering of these CpGs according to their hydroxymethylation signal both in MM patients and in PBs. Hence, a cluster of 415 CpGs uniquely hydroxymethylated in MM was obtained (Supplemental Fig. S3A). A list of 29 genes, including *BMP6* and *FAM72D* (Supplemental Fig. S3B), associating with at least 3 of these hydroxymethylated CpGs was next established and interrogated for prognostic value in the UAMS-TT2 (n=256) and UAMS-TT3 (n=158) Arkansas cohorts (<http://genomicscape.com/>). Interestingly, around a quarter (7/29) of the 29 genes significantly associated with 5hmCpGs were located at 1q21.1 ($p = 7.5e^{-4}$) whereas none were at 1q21.2 (Fig. 3A and

Supplemental Fig. S3C-D). Results showed that among these 29 genes, only 6 had no prognostic value ($p>0.05$) in both analyzed cohorts (Fig. 3A). Others could be classified either as of good ($n=4$) or of poor ($n=7$) prognosis in both cohorts, as exemplified for *FAM72D* (Fig. 3B). Investigating the expression of these genes during differentiation of NBCs, poor prognostic genes were mostly expressed in pre-PBs, whereas good prognostic genes were mainly expressed in non-proliferating cells (Supplemental Fig. S4). Among the poor prognostic genes located on 1q21.1, *FAM72D* is a gene of unknown function which implication in MM biology has not yet been addressed. Of note, recent duplication events of the ancestral *FAM72A* gene led to the presence of 4 highly conserved *FAM72* genes in human (*FAM72A*, *B*, *C*, *D*)³⁹ which cannot be discriminated at the mRNA level (99% identity). Accordingly, "*FAM72*" will be used thereafter when referring to expression data. *FAM72* expression levels correlated with 1q21 copy number, which is associated with poor outcome in MM (Supplemental Fig. S5A-B). Importantly, *FAM72* expression levels correlated with 5hmC enrichment at the *FAM72D* locus (supplemental Fig. S5C) which was not biased by 1q21 amplification (Supplemental Fig. S5D) and was associated with the presence of the enhancer histone modification H3K4me1 in normal plasma cells (Supplemental Fig. S5E). Conversely to *BMP6* (Supplemental Fig. S4 and S5F), expression of *FAM72* was found to be higher in proliferative B cells, *i.e.* centroblasts and pre-PBs (Supplemental Fig. S4), as well as in the Proliferation group (Supplemental Fig. S5G). In accordance with a putative role of *FAM72* in stimulating MM cell proliferation, plasma cell labeling index (PCLI)¹⁹ was significantly correlated with *FAM72* expression in a cohort of 101 newly diagnosed MM patients (Fig. 3C). PCLI was also significantly correlated to *FOXM1* and *CKS1B* expression, but at a lower extent. No correlation was found between MM cell proliferation and *ANP32E* or *ILF2* expression (Fig. 3C). These data suggest that amplification of the 1q21 region, together with its hydroxymethylation, might affect cell proliferation in MM through enhancing *FAM72* expression.

FAM72D is involved in MM cell proliferation

Examination of the top-12 *FAM72* co-expressed ($p<0.05$) genes during NBC differentiation into PCs, highlighted *FOXM1*, a TF known to play a key role in MM cell proliferation⁴⁰ (Fig. 4A). Furthermore, a strong correlation between *FOXM1* and *FAM72* expression was evidenced in MM samples and derived HMCLs (Fig. 4A). ChIP-seq data from GM12878 lymphoblastoid cells indicated that *FOXM1* binds to the *FAM72D* promoter (Supplemental Fig. S6A), strongly suggesting that this TF directly regulates *FAM72D* expression. In support of this hypothesis, *FAM72D* hydroxymethylation levels were positively correlated with *FOXM1* expression (Supplemental Fig. S6B).

Comparison of *FOXM1* and *FAM72* coexpressed genes in patients from the Proliferation molecular MM subgroup revealed a significant overlap (86% of common genes) (Supplemental Fig. S6C). Moreover, *FAM72* co-expressed genes were significantly associated with M phase cell cycle annotations (Supplemental Fig. S6D). *FAM72* was significantly overexpressed in HMCLs and MM cells compared to BMPCs and MGUS, underlining the link with MM cell proliferation (Supplemental Fig. S6E). Furthermore, GSEA analysis of expression data from patients with high *FAM72D* expression and a poor outcome revealed a significant enrichment of genes related to proliferation, overexpressed in proliferating PBs compared to mature BMPCs and stem cell genes (Supplemental Fig. S7). To study the biological function of *FAM72D* overexpression in MM, the XG21 and XG23 HMCLs were selected for their low level of endogenous *FAM72* expression (Supplemental Fig. S8A-B-C). In FCS free medium, *FAM72D* overexpression resulted in significant growth advantage and response to IL-6, a key MM growth factor (Fig. 4B). Similar results were obtained with overexpression of *FAM72D* in XG23 (Supplemental Fig. S8D). These data support the recent characterization of *FAM72B* as an S/G2-M phase gene whose inactivation reduces cell proliferation in human fibroblasts.⁴¹ To test for a FOXM1-dependency of primary cancer cells as well as derived cell lines, FDI-6, a DNA binding inhibitor of FOXM1,⁴² was used. Primary MM cells were highly sensitive to FOXM1 inhibition compared to bone marrow microenvironment cells (Fig. 4C). Overexpression of *FAM72D* in XG21 cells partially counteracted FDI-6-induced cell death (Supplemental Fig. S8E), suggesting that *FAM72D* mediates part of FOXM1 effects on cell growth and survival.

In order to extend our findings to other cancer types, publicly available data were analyzed (<http://www.cbioportal.org/>,⁴³ <https://xenabrowser.net/heatmap/>) and indicated (i) that amplification of 1q21 is a highly prevalent event in breast cancer (Supplemental Fig. S9A) and (ii) a higher expression of *FAM72D* within mutated *TP53* patients (Supplemental Fig. S9B). In agreement with *FAM72* genes being targets of FOXM1, inhibition of FOXM1 in MCF-7 breast cancer cells has been shown to significantly reduce *FAM72D*, *FAM72A* and *FAM72B* expression.⁴⁴ Hence, we next generated genome-wide maps of 5hmC in MCF-7 cells and observed that, as in MM cells, the upstream region of *FAM72D* was highly hydroxymethylated (Supplemental Fig. S9C), suggesting a similar regulation of this gene between MM and breast cancer cells. To investigate a putative function of *FAM72D* in mitosis, *FAM72D* was knocked-down by transfection of siRNAs in MCF-7 cells and mitotic anomalies were analyzed. Data revealed that a reduction in *FAM72D* levels led to a higher occurrence of defects such as misaligned chromosomes, lagging chromatids and micronuclei (Supplemental Fig. S9D), suggesting that *FAM72D* helps maintain mitotic fidelity.

High *FAM72* expression is associated with resistance to Bortezomib and sensitivity to HDACi and DNMTi.

Since *FAM72D* expression is associated with a poor outcome in MM, we investigated whether high *FAM72* expression could be related with drug resistance in MM. Correlating *FAM72* gene expression with response to conventional drugs (bortezomib, melphalan, lenalidomide, dexamethasone and panobinostat) in HMCLs, we identified that high *FAM72* expression levels are associated with resistance to bortezomib ($n=12$, $p=0.049$) (Figure 5A). These observations are consistent with the fact that high *FAM72* expression is associated with a poor prognosis in a cohort of patients at relapse treated by bortezomib mono-therapy (Mulligan cohort, Supplemental Fig. S10A). Conversely, no significant correlation was identified between *FAM72* expression and survival in a cohort of patients at relapse treated by dexamethasone mono-therapy (Supplemental Fig. S10B) and between *FAM72* expression and *in vitro* HMCL response to melphalan, lenalidomide or dexamethasone (not shown). Of particular interest, high *FAM72* expression tended to be significantly correlated with a better response to panobinostat ($n=10$, $p=0.061$; Supplemental Fig. S10C), suggesting that HDACi could have a therapeutic interest in *FAM72*^{high} myeloma patients associated with poor survival. Since a combination of both HDAC and DNMT inhibitors has been shown to reprogram HMCL cells,⁴⁵ we next investigated the ability of the combined DNMT and HDAC inhibitors decitabine (5aza-dC) and trichostatin A (TSA) to regulate *FAM72* and *FOXM1* expression in HMCLs. Data indicated that the combined treatment reduced, although to different extent, the expression of both genes in a majority of investigated cell lines (Fig. 5B). Finally, primary MM cells were treated with a similar combination (5aza-C and SAHA) and their resistance to these drugs was inversely correlated to the expression of *FAM72* and *FOXM1* (Fig. 5C and Supplemental Fig. S10D). When considering *FAM72*^{high}/*FAM72*^{low} and *FOXM1*^{high}/*FOXM1*^{low} expressing cells, only *FAM72*^{high} samples remained significantly correlated with higher sensitivity to the HDCAi/DNMTi combination (Fig. 5C). These results suggest that high-risk patients overexpressing *FAM72* could benefit from treatment by a HDACi/DNMTi combination.

Discussion

Collectively, our data point to a prominent role of DNA demethylation events occurring at 1q21.1, and specially at the *FAM72D* locus, in MM biology and malignancy. One of the most common genetic features in MM linked to high-risk prognosis is the gain (3 copies) or amplification (4 and more copies) of part or all of the q arm of chromosome 1.⁴⁶ Among the partial gains of 1q, 1q21 is particularly detected both in newly diagnosed (30%)

and relapse (70%) cases. However, there is still no unifying picture explaining the functional role of 1q arm amplification and its wide occurrence among high-risk patients. Interestingly, MM-like 1q alterations can be experimentally triggered by inhibiting DNA methylation. Indeed, 5aza-dC treatment of activated B cells leads to a decondensation of 1q12 pericentromeric chromatin, a process that might enable local rearrangements of the 1q arm.⁴⁷ Although DNA methylation levels are generally low in MM cells, residual methylation accumulates at specific sites¹⁷ and can still be erased by active demethylation through TET enzymes. Such mechanisms could play a role in disease progression provided that TETs are targeted to the pericentromeric region of chromosome 1 and its adjacent region 1q21. Consistent with this idea, we show that one fourth of the genes associated with MM-specific hydroxymethylated regions lie within the 1q21.1 region. Among them, *FAM72D*, a gene encoding for a protein of unknown function, was shown here to enhance proliferation of MM cells. Whereas most mammals have only one copy of the *FAM72* gene, due to recent duplication events, four genes encode the human *FAM72* proteins A to D.³⁹ The *FAM72* genes are known to be overexpressed in cancer and favor tumorigenesis induced by the Epstein-Barr virus-derived latent membrane protein 1.^{48,49} *FAM72* genes are highly expressed in *TP53* mutated cancer cells, whose growth has been shown to be dependent on *FAM72D*.^{50,51} Interestingly, cancer cell growth dependency on *FAM72D* has also been demonstrated for cells with mutated or copy number variants of *p300*, *p19Arf* and *CDK12A*,⁵¹ suggesting that *FAM72D* is required for the growth of different cancer types. Corroborating the tumorigenic potential of *FAM72* proteins, two insertional mutagenesis screens in mouse identified the mouse *SRGAP2/FAM72A* locus as a driver of chronic myeloid leukemia progression and growth factor-independent leukemogenesis.^{52,53} Hence, TET-mediated demethylation of the *FAM72D* upstream region is likely coupled to the proliferation potential of MM cells.

We have defined here a MM-specific hydroxymethylome that favors a survival/proliferation program relying, at least in part, on the cooperative actions of enhancers and super-enhancers controlling *FAM72D*, *GAS2*, *DEPTOR* and *MYC* expression (Fig. 6). In accordance with the observation that *FAM72* expression is predictive to the sensitivity of MM cells to different treatments, its evaluation in patients could help to tailor therapy.

Acknowledgements

GS was supported by a grant from La Ligue Contre le Cancer (Grand Ouest committee). The work was partially funded by the hematology laboratory of Rennes University Hospital. AP was supported by PhD training grants

from Région Bretagne and Ligue Nationale Contre le Cancer. JM was supported by grants from French INCA (Institut National du Cancer) Institute (PLBIO15-256), PLBIO2018-PIT-MM, LR-FEDER Hemodiag, Fondation de France (201400047510), ITMO Cancer (MM&TT), SIRIC Montpellier (INCa-DGOS-Inserm 6045) and Labex EpiGenMed. The authors thank the BioGenouest GEH sequencing platform (<https://geh.univ-rennes1.fr/>) from the UMS Biosit.

Conflict of Interests

The authors declare that they have no competing interests.

References

1. Zhan F, Huang Y, Colla S, et al. The molecular classification of multiple myeloma. *Blood*. 2006;108(6):2020-2028.
2. Bolli N, Avet-Loiseau H, Wedge DC, et al. Heterogeneity of genomic evolution and mutational profiles in multiple myeloma. *Nat Commun*. 2014;5:2997.
3. Lohr JG, Stojanov P, Carter SL, et al. Widespread genetic heterogeneity in multiple myeloma: implications for targeted therapy. *Cancer Cell*. 2014;25(1):91-101.
4. Delmore JE, Issa GC, Lemieux ME, et al. BET bromodomain inhibition as a therapeutic strategy to target c-Myc. *Cell*. 2011;146(6):904-917.
5. Moreaux J, Reme T, Leonard W, et al. Gene expression-based prediction of myeloma cell sensitivity to histone deacetylase inhibitors. *Br J Cancer*. 2013;109(3):676-685.
6. Herviou L, Kassambara A, Boireau S, et al. PRC2 targeting is a therapeutic strategy for EZ score defined high risk multiple myeloma patients and overcome resistance to IMiDs. *Clin Epigenetics*. 2018;10(1):121.
7. Sawyer JR, Tricot G, Mattox S, Jagannath S, Barlogie B. Jumping translocations of chromosome 1q in multiple myeloma: evidence for a mechanism involving decondensation of pericentromeric heterochromatin. *Blood*. 1998;91(5):1732-1741.
8. Hanamura I, Stewart JP, Huang Y, et al. Frequent gain of chromosome 1q21 in plasma-cell dyscrasias detected by fluorescence in situ hybridization: incidence increases from MGUS to relapsed myeloma and is related to prognosis and disease progression following tandem stem-cell transplantation. *Blood*. 2006;108(5):1724-1732.

9. Walker BA, Leone PE, Chiecchio L, et al. A compendium of myeloma-associated chromosomal copy number abnormalities and their prognostic value. *Blood*. 2010;116(15):e56-65.
10. Marchesini M, Ogoti Y, Fiorini E, et al. ILF2 is a regulator of RNA splicing and DNA damage response in 1q21 amplified multiple myeloma. *Cancer Cell*. 2017;32(1):88-100.
11. Paiva B, Puig N, Cedena MT, et al. Differentiation stage of myeloma plasma cells: biological and clinical significance. *Leukemia*. 2017;31(2):382-392.
12. Wu X, Zhang Y. TET-mediated active DNA demethylation: mechanism, function and beyond. *Nat Rev Genet*. 2017;18(9):517-534.
13. Sérandour AA, Avner S, Oger F, et al. Dynamic hydroxymethylation of deoxyribonucleic acid marks differentiation-associated enhancers. *Nucleic Acids Res*. 2012;40(17):8255-8265.
14. Caron G, Hussein M, Kullis M, et al. Cell-cycle-dependent reconfiguration of the DNA methylome during terminal differentiation of human B cells into plasma cells. *Cell Rep*. 2015;13(5):1059-1071.
15. Lio C-W, Shukla V, Samaniego-Castruita D, et al. TET enzymes augment activation-induced deaminase (AID) expression via 5-hydroxymethylcytosine modifications at the *Aicda* superenhancer. *Sci Immunol*. 2019;4(34).
16. Jin Y, Chen K, De Paepe A, et al. Active enhancer and chromatin accessibility landscapes chart the regulatory network of primary multiple myeloma. *Blood*. 2018;131(19):2138-2150.
17. Agirre X, Castellano G, Pascual M, et al. Whole-epigenome analysis in multiple myeloma reveals DNA hypermethylation of B cell-specific enhancers. *Genome Res*. 2015;25(4):478-487.
18. Viziteu E, Klein B, Basbous J, et al. RECQ1 helicase is involved in replication stress survival and drug

- resistance in multiple myeloma. *Leukemia*. 2017;31(10):2104-2113.
19. Requirand G, Robert N, Boireau S, et al. BrdU incorporation in multiparameter flow cytometry: A new cell cycle assessment approach in multiple myeloma. *Cytometry B Clin Cytom*. 2019;96(3):209-214.
20. Barlogie B, Tricot G, Rasmussen E, et al. Total therapy 2 without thalidomide in comparison with total therapy 1: role of intensified induction and posttransplantation consolidation therapies. *Blood*. 2006;107(7):2633-2638.
21. Pineda-Roman M, Zangari M, Haessler J, et al. Sustained complete remissions in multiple myeloma linked to bortezomib in total therapy 3: comparison with total therapy 2. *Br J Haematol*. 2008;140(6):625-634.
22. Mulligan G, Mitsiades C, Bryant B, et al. Gene expression profiling and correlation with outcome in clinical trials of the proteasome inhibitor bortezomib. *Blood*. 2007;109(8):3177-3188.
23. Song CX, Szulwach KE, Fu Y, et al. Selective chemical labeling reveals the genome-wide distribution of 5-hydroxymethylcytosine. *Nat Biotechnol*. 2011;29(1):68-72.
24. Sérandour AA, Avner S, Mahé EA, et al. Single-CpG resolution mapping of 5-hydroxymethylcytosine by chemical labeling and exonuclease digestion identifies evolutionarily unconserved CpGs as TET targets. *Genome Biol*. 2016;17:56.
25. Sérandour AA, Avner S, Salbert G. Coupling exonuclease digestion with selective chemical labeling for base-resolution mapping of 5-hydroxymethylcytosine in genomic DNA. *Bio Protoc*. 2018;8(5):2747.
26. Liu T, Ortiz JA, Taing L, et al. Cistrome: an integrative platform for transcriptional regulation studies. *Genome Biol*. 2011;12(8):R83.
27. Zhang Z, Chang CW, Goh WL, Sung WK, Cheung E. Centdist: discovery of co-associated factors by motif

- distribution. *Nucleic Acids Res.* 2011;39(Web Server issue):W391-399.
28. McLean CY, Bristor D, Hiller M, et al. GREAT improves functional interpretation of cis-regulatory regions. *Nat Biotechnol.* 2010;28(5):495-501.
29. Stewart SK, Morris TJ, Guilhamon P, et al. oxBS-450K: a method for analysing hydroxymethylation using 450K beadchips. *Methods.* 2015;72:9-15.
30. Shaffer AL, Emre NC, Lamy L, et al. 2008. IRF4 addiction in multiple myeloma. *Nature.* 2008;454(7201):226-231.
31. Liu Z, Xu J, He J, et al. A critical role of autocrine sonic hedgehog signaling in human CD138+ myeloma cell survival and drug resistance. *Blood.* 2014;124(13):2061-2071.
32. Jundt F, Probsting KS, Anagnostopoulos I, et al. Jagged1-induced Notch signaling drives proliferation of multiple myeloma cells. *Blood.* 2004;103(9):3511-3515.
33. Cai L, Langer EM, Gill JG, et al. Dual actions of Meis1 inhibit erythroid progenitor development and sustain general hematopoietic cell proliferation. *Blood.* 2012;120(2):335-346.
34. Lovén J, Hoke HA, Lin CY, et al. Selective inhibition of tumor oncogenes by disruption of super-enhancers. *Cell.* 2013;153(2):320-334.
35. Peterson TR, Laplante M, Thoreen CC, et al. DEPTOR is an mTOR inhibitor frequently overexpressed in multiple myeloma cells and required for their survival. *Cell.* 2009;137(5):873-886.
36. Zhou H, Ge Y, Sun L, et al. Growth arrest specific 2 is up-regulated in chronic myeloid leukemia cells and required for their growth. *PLoS One.* 2014;9(1):e86195.

37. Maupetit-Methouas S, Court F, Bourgne C, et al. DNA methylation profiling reveals a pathological signature that contributes to transcriptional defects of CD34+ CD15- cells in early chronic-phase chronic myeloid leukemia. *Mol Oncol*. 2018;12(6):814-829.
38. Wang Y, Zhang Y. Regulation of TET protein stability by calpains. *Cell Rep*. 2014;6(2):278-284.
39. Kutzner A, Pramanik S, Kim PS, Heese K. All-or-(N)One - an epistemological characterization of the human tumorigenic neuronal paralogous FAM72 gene loci. *Genomics*. 2015;106(5):278-285.
40. Gu C, Yang Y, Sompallae R, et al. FOXM1 is a therapeutic target for high-risk multiple myeloma. *Leukemia*. 2016;30(4):873-882.
41. Giotti B, Chen S-H, Barnett MW, et al. Assembly of a parts list of the human mitotic cell cycle machinery. *J Mol Cell Biol*. 2018 Nov 17. [Epub ahead of print]
42. Gormally MV, Dexheimer TS, Marsico G, et al. Suppression of the FOXM1 transcriptional programme via novel small molecule inhibition. *Nat Commun*. 2014;5:5165.
43. Gao J, Aksoy BA, Dogrusoz U, et al. Integrative analysis of complex cancer genomics and clinical profiles using cBioPortal. *Sci Signal*. 2013;6(269):p1.
44. Sanders DA, Ross-Ines CS, Beraldi D, Carroll JS, Balasubramanian S. Genome-wide mapping of FOXM1 binding reveals co-binding with estrogen receptor alpha in breast cancer cells. *Genome Biol*. 2013;14(1):R6.
45. Bruyer A, Maes K, Herviou L, et al. DNMTi/HDACi combined epigenetic targeted treatment induces reprogramming of myeloma cells in the direction of normal plasma cells. *Br J Cancer*. 2018;118(8):1062-1073.
46. Pawlyn C, Morgan GJ. Evolutionary biology of high-risk multiple myeloma. *Nat Rev Cancer*. 2017;17(9):543-

556.

47. Sawyer JR, Tian E, Heuck CJ, et al. Evidence of an epigenetic origin for high-risk 1q21 copy number alterations in multiple myeloma. *Blood*. 2015;125(24):3756–3759.
48. Guo C, Zhang X, Fink SP, et al. Ugene, a newly identified protein that is commonly overexpressed in cancer and binds uracil DNA glycosylase. *Cancer Res*. 2008;68(15):6118-6126.
49. Wang LT, Lin CS, Chai CY, Liu KY, Chen JY, Hsu SH. Functional interaction of Ugene and EBV infection mediates tumorigenic effects. *Oncogene*. 2011;30(26):2921-2932.
50. Wang X, Sun Q. TP53 mutations, expression and interaction networks in human cancers. *Oncotarget*. 2017;8(1):624-643.
51. Tshemiak A, Vazquez F, Montgomery PG, et al. Defining a cancer dependency map. *Cell*. 2017;170(3):564-576.
52. Giotopoulos G, van der Weyden L, Osaki H, et al. A novel mouse model identifies cooperating mutations and therapeutic targets critical for chronic myeloid leukemia progression. *J Exp Med*. 2015;212(10):1551-1569.
53. Guo Y, Updegraff BL, Park S, et al. Comprehensive Ex vivo transposon mutagenesis identifies genes that promote growth factor independence and leukemogenesis. *Cancer Res*. 2016;76(4):773-786.

FIGURE LEGENDS

Figure 1: Analysis of the hydroxymethylome of multiple myeloma. (A) Molecular classification of the patient samples analyzed in this study. HMCL indicates the names of cell lines derived from patient samples. The molecular groups are based on Zhan et al¹. MM: multiple myeloma, BM: bone marrow, PCL: plasma cell leukemia. (B) Principal component analysis (PCA) of 5hmC distribution either in all MM patients, compared to NBCs and PBs (left), or in the subset of MM patients from the CCND1, MMSET and Proliferation groups. Clusters 1, 2 and 3 (C1, C2 and C3) group samples with similar 5hmC distribution. (C) Heatmap clustering of the SCL-seq signal in C1 to C3 patients at the union of overlapping 5hmCpGs and Functional annotation with GREAT of genes associated with C'1 and C'2 5hmCpGs. For each annotation, the corresponding *p* value is indicated.

Figure 2: Genomic and epigenomic characterization of sites of 5mC oxidation in MMPCs. (A) CEAS³¹ analysis of the distribution of high confidence MM 5hmCpGs (n=86,591) and Box plot comparing expression levels of genes associated or not with 5hmC peaks in MM patients. (B) Heatmap representation of H3K4me1 and H3K27ac ChIP-seq signals at MM 5hmCpGs. NBC and PC H3K4me1 data were from the Blueprint consortium (<http://dcc.blueprint-epigenome.eu/#/files>), and MM H3K27ac data were downloaded from the European Nucleotide Archive (PRJEB25605). (C) Integrated genome browser (IGB) visualization of H3K4me1 from normal plasma cells (PC H3K4me1), 5hmC from in vitro differentiated plasmablasts (PB 5hmC), MM 5hmCpGs and SCL-exo signal from E10025 at selected super enhancers active in MM1.S cells. The survival of patients from the Arkansas cohort classified as high (n=71) or low (n=343) *GAS2* expression is shown on the right.

Figure 3: A multiple myeloma-specific hydroxymethylation signature uncovers new prognostic genes. (A) Genes associated with at least 3 MM-specific 5hmCpGs were analyzed with Genomic-Scape 2.0 for their prognostic value in two cohorts of patients (Arkansas TT2 and TT3). Genes associated with good prognosis are indicated in green and genes associated with poor prognosis in red. The associated *p*-values are also indicated with the same color code. Cutoff was set at *p*=0.05. (B) Overall survival of patients from the TT2 Arkansas cohort expressing low (blue curves) or high (red curves) levels of *FAM72D* (lower panels). (C) Correlations between PCL scores and gene expression values in a cohort of 101 patients.

Figure 4: FAM72D regulates cell proliferation in multiple myeloma. (A) Analysis of *FAM72* co-expressed genes

during B cell differentiation in naive B cells (NBCs), centroblasts (CBs), centrocytes (CCs), memory B cells (MBCs), pre-plasmablasts (prePBs), plasmablasts (PBs), early plasma cells (early PCs), and bone marrow plasma cells (BMPCs). Only the Top-12 co-regulated genes are shown. *FOXM1* ranked at position 11. Graph on the right shows the correlation between *FAM72* and *FOXM1* gene expression in the MM patients and derived cell lines for which 5hmCpGs were mapped by SCL-exo. (B) Proliferation assay of XG21 (blue bars) and XG21-FAM72D (orange bars) cells in the presence of increasing concentrations of IL-6. (C) Impact of increasing concentrations of the FOXM1 inhibitor FDI-6 on the *in vitro* growth of bone marrow cells from MM patients (n=6).

Figure 5: *FAM72* expression levels predict MM cell sensitivity to drugs. (A) 12 HMCLs were cultured with graded concentrations of Bortezomib for 4 days and IC50 were calculated with mean values of five experiments determined on sextuplet culture wells. High *FAM72* expression (Affymetrix microarrays) was significantly correlated with resistance to Bortezomib. (B) HDACi/DNMTi induce a significant downregulation of *FAM72* and *FOXM1* in MM. Nine HMCLs were treated for 7 days with decitabine (DNMTi) and TSA during the last 24 hours and gene expression was assessed using Affymetrix U133P microarrays. (C) *FAM72* expression predicts 5-azacytidine/SAHA combination sensitivity of primary myeloma cells of patients. Mononuclear cells from tumor samples of 17 patients with MM were cultured for 4 days in the presence of IL-6 (2 ng/ml) with or without 2 μ M 5-azacytidine and 300 nM SAHA. At day 4 of culture, the count of viable MMCs was determined using CD138 staining by flow cytometry. Samples from Fig. 6C and Supplemental Fig. S10C were grouped as *FAM72*high or low and *FOXM1*high or low and correlation coefficients between *FAM72* or *FOXM1* expression and the percentage of living MM cells were calculated with GraphPad Prism.

Figure 6: 5mC oxidation at *FAM72D* enhancer and *GAS2*, *DEPTOR* and *MYC* super enhancers associate with MM. 5mC oxidation in MM cells occurs at SEs and normal enhancers and as such participates in the establishment of an MM-specific transcription program and the maintenance of plasma cell identity. Several scenarios may lead to *FAM72D* overexpression in MM, including 1q21 gain/amplification, FOXM1 upregulation and DNA demethylation, and might combine in high risk MM to enhance survival and proliferation.

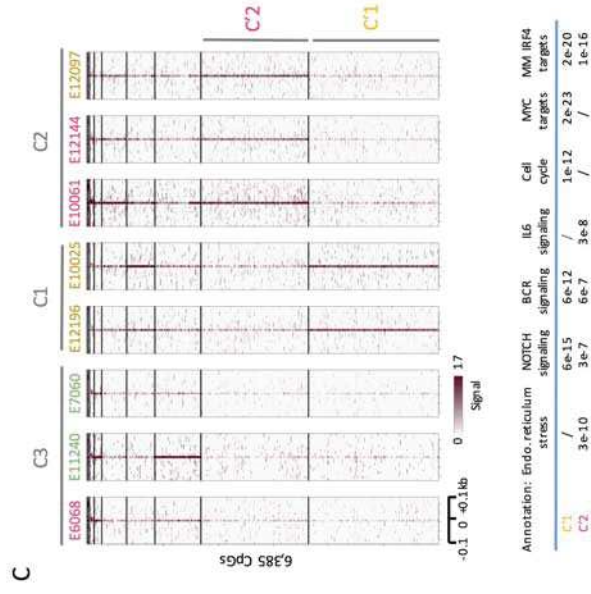
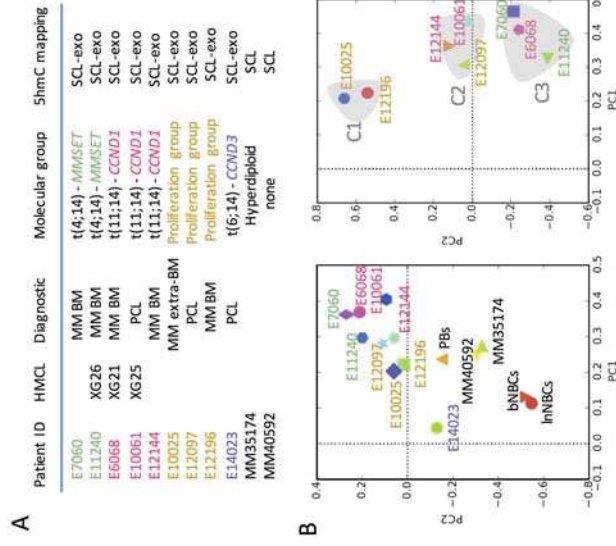


Fig. 1

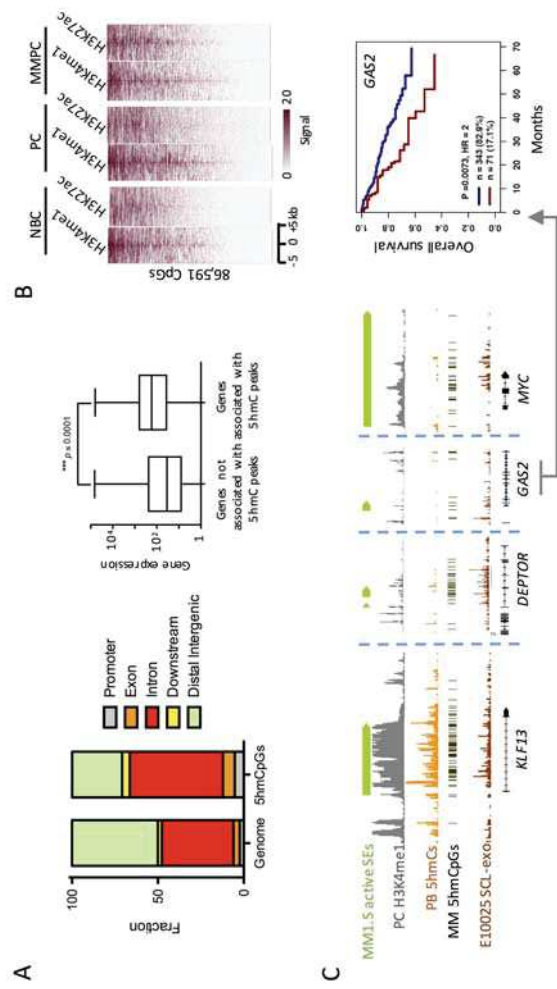


Fig. 2

A

GENE NAME	Localization	Cohort p value	
		TTZ (n=256)	TT3 (n=158)
NOTCH2	1p12-1p11.2	6.9e-3	ns
CD160	1q21.1	ns	ns
FAM72D	1q21.1	3.1e-7	2.7e-4
GPR88A	1q21.1	1.5e-4	3.6e-3
NOTCH2NL	1q21.1	ns	ns
PDE4DIP	1q21.1	5.8e-3	8.8e-3
PDZK1	1q21.1	ns	ns
SEC22B	1q21.1	ns	1.9e-3
LINC00152	2p11.2	3.3e-4	0.011
FRG1	4q35.2	ns	0.019
BMP6	6q24.3	2.3e-3	7.3e-5
RSPH10B	7p22.1	0.017	ns
GTF2IRD2	7q11.23	0.045	7.4e-3
GTF2IRD2B	7q11.23	0.047	ns
NCF1C	7q11.23	0.023	0.017
ARHGEF34P	7q35	ns	ns
CTAGE4	7q35	ns	0.015
DR2AZ0P	7q35	1.3e-3	ns
MIR1204	8q24.21	0.013	0.034
TMEM75	8q24.21	0.027	ns
KIAA1217	10p12.1	6.7e-3	8.3e-5
GOLGA8A	15q13.1	9.1e-3	ns
HERC2P9	15q13.1	ns	ns
EF3C	16p11.2	3.7e-3	5.7e-3
CDK2	16p12.2	ns	ns
NPIP5	16p12.2	0.02	7.6e-3
RRNBP3	16p12.2	6.2e-3	ns
USP14	18p11.32	2.9e-6	2.4e-4

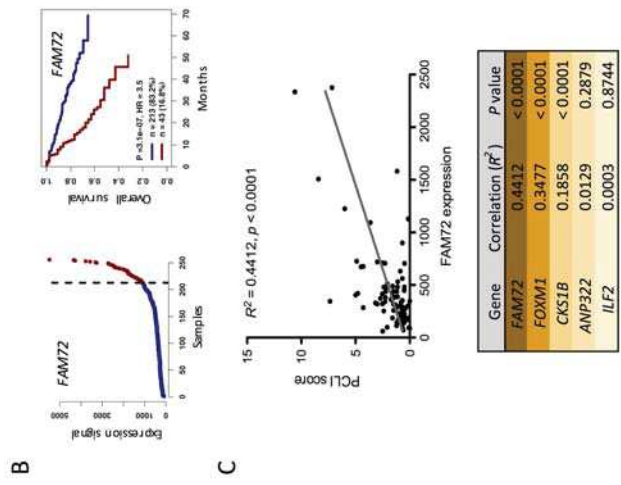


Fig. 3

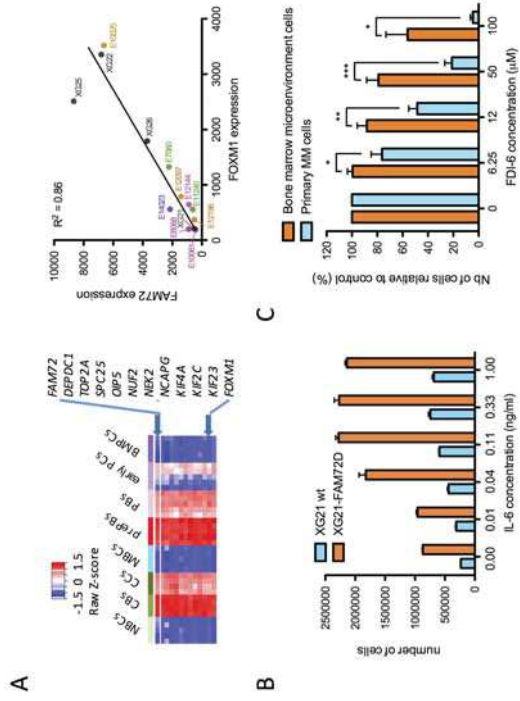


Fig. 4

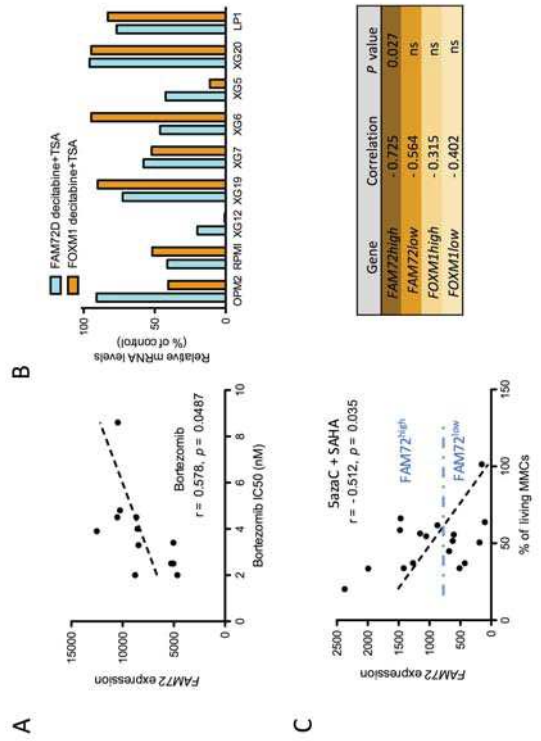


Fig. 5

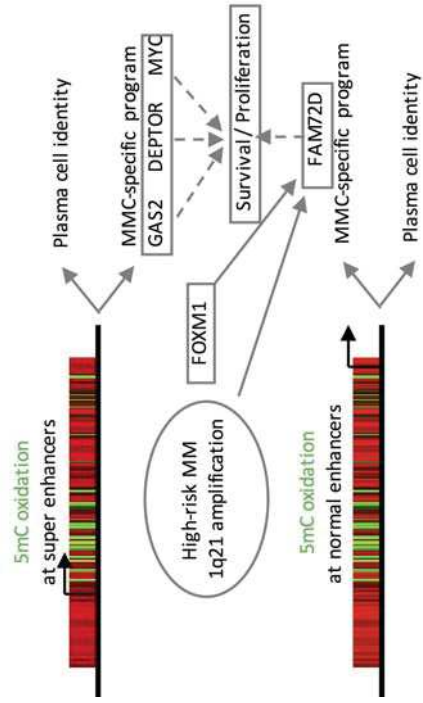


Fig. 6